Journal of Applied Polymer Science

Monodispersed Composite Particles Prepared via Emulsifier-Free Emulsion Polymerization Using Waterborne Polyurethane as Microreactors

Wenna Zhuge, Mingwang Pan, Yanning Chang, Jinfeng Yuan, Xiaomei Wang, Caili Sun, Guanglin Zhang

Institute of Polymer Science and Engineering, Hebei University of Technology, Tianjin 300130, People's Republic of China

Correspondence to: M. W. Pan (E-mail: mwpan@126.com)

ABSTRACT: Monodispersed polystyrene particles in submicrometer size were intriguingly prepared through emulsifier-free batch-seeded emulsion polymerization using nonmonodispersed waterborne polyurethane (WBPU) beads as microreactors. Different feed ratios of styrene (St)/WBPU for the preparation of composite particles were investigated, and the size–growth course was experimentally followed. The morphology and dispersity of the particles were characterized by scanning electron microscopy together with dynamic laser scattering particle size analyzer. Their inside structure was further characterized by transmission electron microscopy with ultramicrotomy combined with X-ray photoelectron spectroscopy for the composite particles' surface analysis. The probable grafting polymerization of St from WBPU was verified by Fourier transform infrared spectroscopy and nuclear magnetic resonance instrument. The obtained composite particles were again employed as the seeds in the emulsion copolymerization of methyl methacrylate. As a result, the formed multilayered composite particles with reverse core–shell structure were also monodispersed and spherical. The mechanism of the formation of the monodispersed particles was proposed. © 2014 Wiley Periodicals, Inc. J. Appl. Polym. Sci. **2014**, *131*, 40985.

KEYWORDS: emulsion polymerization; latices; morphology; polyurethanes

Received 27 December 2013; accepted 7 May 2014

DOI: 10.1002/app.40985

INTRODUCTION

Spherical polymeric nano- and microspheres have received considerable attention for their potential applications in photonic crystals, medical field, lithography, and as the templates for other periodic structures ranging.[1–7] Dow Chemical Corporation in 1947 was the first to demonstrate the synthesis of monodispersed polystyrene (PS) latex colloids. This study was followed by the development of additional synthetic approaches that produce monodispersed colloidal particles including miniemulsion polymerization, emulsion polymerization, seeded emulsion polymerization, emulsifier-free emulsion polymerization, precipitation polymerization, and dispersion polymerization.[2,8–21] Winnik and coworkers[22] discovered, in the dispersion polymerization of St in ethanol, that if a crosslinking agent was added at the end of the nucleation stage, the crosslinked particles with a very narrow size distribution could be obtained successfully. The two-stage swelling method has been widely used to synthesize uniform polymer beads efficiently.[13,17,20] These monodispersed particles can form highly ordered, compact structures that diffract light.[10]

In addition to the abovementioned polymerization methods, there are some novel methods for the synthesis of monodispersed particles recently. A versatile strategy for generating the monodisperse solid particles from 20 to 1000 μm is to utilize microfluidics to control their sizes, shapes, and compositions. This method involves the formation of monodisperse liquid droplets by using a microfluidic device and shaping the droplets in a microchannel and then solidifying these drops *in situ* either by polymerizing a liquid monomer or by lowering the temperature of a liquid that sets thermally.[23] Another method is a very rapid procedure based on the photoinitiated free radical polymerization owing to its temperature insensitivity. The reaction can be carried out at room temperature or even lower.[24]

Particles with submicrometer dimensions are mostly prepared by emulsion polymerization. Emulsifier-free emulsion polymerization is particularly effective for preparing functional polymer particles with a very narrow diameter distribution in the range of 300–800 nm and submicrometer anisotropic particles with special function.[20,25] In addition, the latex particles produced by emulsifier-free emulsion polymerization contain no low molecular weight of emulsifier which can affect application performance of the latex particles.

As a matter of fact, waterborne polyurethane (WBPU) system is a typical emulsifier-free emulsion polymerization system. In recent

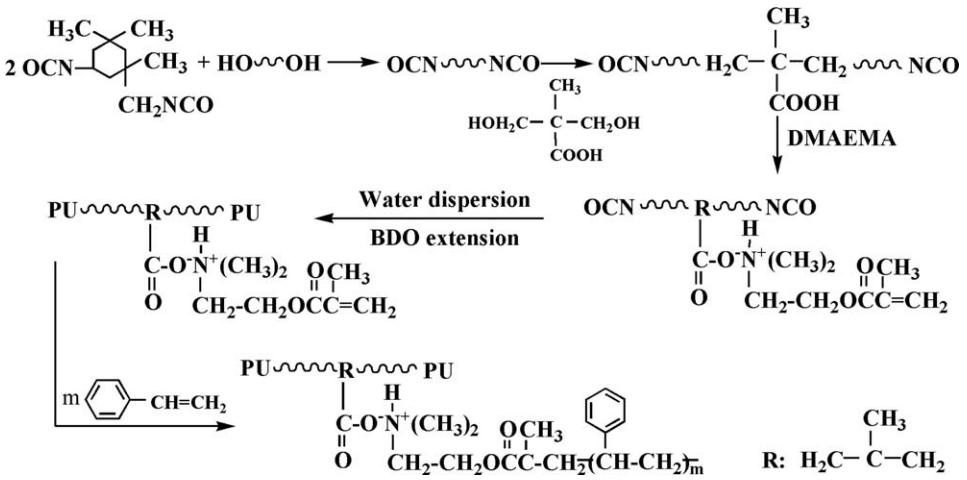

Scheme 1. Schematic diagram of the synthesis of WBPU and grafting of PS from WBPU.

report on work, WBPU was often used as the stabilizer for the preparation of PS/WBPU and poly(methyl methacrylate) (PMMA)/WBPU composite latex particles through ray or free radical-initiated miniemulsion polymerization, and dispersion polymerization.[15,24,26–28] It is significant that the individual properties of composite particles can be tailored by changing the average size and composition for alloy systems. Recently, the latter step has been actively investigated as alloy core–shell composite particles are ideal multifunctional structures in which shell and core provide different, sometimes synergistic functions.[29]

In this study, we first synthesized the WBPU/PS composite particles using nonmonodisperse WBPU beads as seed latex. We tried to focus on the control over the composite particle size and morphology, and further research the phase separation of both WBPU and PS derived from their incompatibility.[25] Next, we found that the obtained composite particles were monodispersed and within submicrometer size. Then, we investigated the morphology and the growing process of the composite particles on the basis of the intriguing experimental results.

The particles prepared in this study have unique properties. For example, their surfaces can be easily modified with functional groups in polyurethane for desired properties, because many functional comonomers (such as double bond, amine, hydroxyl, or other functional groups) can be easily introduced by polyaddition reaction of synthesis polyurethane, which endows excellent abrasion resistance and properties of both rubber and plastics. In addition, layer-by-layer composite particles are expected using our synthetic method.

These novel monodispersed composite particles may have great potentials as the additives to improve the properties of materials. For instance, the mechanical performance of a soft polymer can be effectively enhanced through the addition of such hard fillers. Nano- and microparticles are especially advantageous because of relatively large interfacial regions between the polymer and the particles inside the composite. The large interfacial regions facilitate the stress transfer between the soft matrix and the stiffer inclusions, which plays a crucial role in determining the mechanical properties of the material.[30]

EXPERIMENTAL

Materials

The polyester diol (218 type, industrial product, Xuzhou Xinxin Chemical Plant) was dehydrated under reduced pressure. 2,2-*Bis*(hydroxymethyl) propionic acid (DMPA, industrial product, Huzhou Changsheng Chemical) was dried under reduced pressure for 2 h at 110°C. St, divinylbenzene (DVB), and methyl methacrylate (MMA) (AR, Tianjin Chemical Reagent) were distilled under reduced pressure to remove inhibitors. The purified St, DVB, and MMA were stored in a freezer prior to use. Dimethyl formamide (DMF, AR, Tianjin Bodi Chemical) was dried with molecular sieve. Dimethylaminoethyl methacrylate (DMAEMA, CP, Zibo Wanduofu Chemical), isophorone diisocyanate (IPDI, CP, Tianjin Chemical Reagent), potassium persulfate ($K_2S_2O_8$, AR, China Medicine Group Chemical Reagent), and 1, 4-butanediol (BDO, AR, Tianjin Chemical Reagent) were used without further purification.

Preparation of WBPU Colloidal Particles

The WBPU was synthesized as shown in Scheme 1. The polymerization reactions were carried out in a 250 mL of four-necked round-bottomed flask equipped with a condenser, a polytetrafluoroethylene stirrer, and a nitrogen inlet. In brief, 20.0 g of IPDI and 50.0 g of polyester diol (218 type) were added into the reactor and heated to 80°C for 1 h; 4.0 g of DMPA dissolved in 8.0 g of DMF was added to the mixture, and the prepolymerization was proceeded at 80°C for 1.5 h. The prepolymer was cooled to 60°C and then neutralized with DMAEMA. The WBPU aqueous dispersion was obtained by adding water, drop by drop, and chain-extension process with 2.0 g of BDO aqueous solution was continued by a dispersion machine at 1000 rpm for 1.5 h.

Preparation of WBPU/PS Composite Particles

The WBPU/PS composite particles were synthesized by emulsifier-free batch-seeded emulsion polymerization. All polymerization reactions were carried out at 70°C in a 250-mL four-necked round-bottomed flask equipped with a condenser, a polytetrafluoroethylene stirrer, and a nitrogeninlet. First, 4.0 g of WBPU dispersion with a solid content of about 25 wt % was

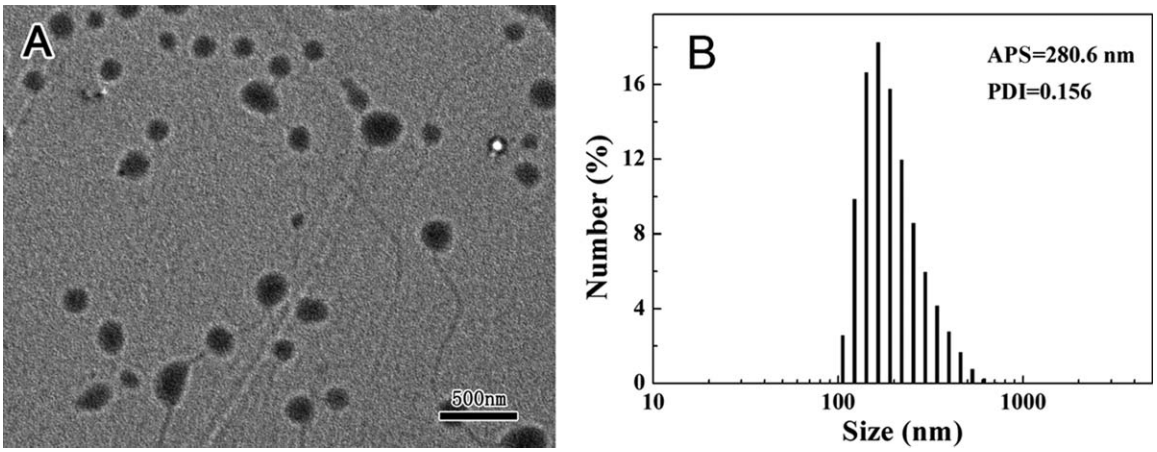

Figure 1. (A) TEM micrograph of the WBPU latex particles and (B) particle size distribution histogram of the WBPU latex particles.

added into the above flask containing 90.0 g of deionized water at room temperature. Then 10.0 g (or 20.0 g) of the purified St monomer was added in one batch into the flask. The mixture was agitated for 2 h to let the St monomer penetrate inside the WBPU colloidal particles at room temperature, followed by heating to 70°C. Then, a 6 mL of aqueous solution containing 0.06 g of $K_2S_2O_8$ (i.e., 0.6 wt % of the St monomer) was added into the mixture, and polymerization reaction was kept at 70°C for 5 h until the conversion of St reached about 60 wt %.

Preparation of (WBPU/PS)/PMMA Composite Particles

The procedure was the same as the WBPU/PS composite particles. The WBPU/PS composite latex was used for seed latex after unreacted St monomer was removed through distillation under reduced pressure for 1 h.

Characterization

The size distributions of pure WBPU particles and composite particles in aqueous dispersions were analyzed by Zeta-Sizer 90 type of dynamic laser scattering particle size analyzer (Malvern, England). The WBPU/PS composites were extracted by acetic acid for 72 h using Soxhlet's apparatus to remove unhybrided WBPU physically absorbed on the surface of PS particles, and then dried in vacuum at room temperature after washed with distilled water at least three times. The eventually obtained particles were used for infrared scanning. The infrared spectra were recorded with Fourier transform infrared spectroscopy (FTIR, Tensor-27, Bruck, Germany). The nitrogen content on the surface of the composite particles was performed by X-ray photoelectron spectroscopy (XPS, Genesis 60S, EDAX, USA). ^{1}H nuclear magnetic resonance (NMR) spectra were performed using an Avance400 NMR instrument (Bruker Biospin AG) to confirm the occurrence of probable grafting between WBPU and PS. Typically, a small amount of WBPU dry film or WBPU/PS particles sample was dissolved in 0.5 mL of deuterochloroform, then after removing crosslinked PS, the ^{1}H NMR spectra were recorded at room temperature.

Morphology Observation of Composite Particles. ***Scanning electron microscopy.*** Morphology and size distribution of WBPU/PS and (WBPU/PS)/PMMA composite particles were also studied by scanning electron microscopy (SEM, JSM-6500F, JEOL, Japan). Typically, a drop of the WBPU/PS latex sampled at a preset time interval without special purification was diluted with 2.5 mL of deionized water to obtain a translucent solution. After ultrasonication for 10 min, a drop of the suspension was cast onto a small conductive silicon wafer, and the wafer was dried at room temperature under a reduced pressure overnight. Then, the sample was sprayed by sputter coater (SC7620, Quorum, England) for 40 s.

Transmission electron microscopy. Morphologies of WBPU/PS and (WBPU/PS)/PMMA composite particles were studied by transmission electron microscopy (TEM, H-7650B, Hitachi, Japan). Few particles were embedded in melted epoxy resin, which was solidified at 60°C for 2 days. The particles were sectioned in the ultramicrotome according to the procedure used in electron microscopy. The samples were stained by osmium tetraoxide (OsO_4) for 2 h, and the thickness of sections was around 70 nm.

Dynamic Mechanical Analysis

Dynamic mechanical analysis (DMA) was performed on a Netzsch DMA242 type of dynamic mechanical analyzer (Germany). The measuring frequency was 1 Hz; the heating rate was 3 K/min; and the range of scanning temperature was from −110 to 200°C. The size of the samples for the DMA test was 40 × 7 × 2 (height × width × thickness) mm^3. The samples were manufactured using composite particle powder by hot-press molding except for the WBPU film prepared at reduced pressure.

RESULTS AND DISCUSSION

Morphology and Structure Study of WBPU/PS Composite Particles

Figure 1 shows the particle morphology and size distribution of the WBPU dispersion obtained by SEM observation and particle size analysis, respectively. The number-average particle size (APS) was determined to be ~280 nm and the polydispersity index (PDI) was 0.156 [Figure 1(B)]. As shown in Figure

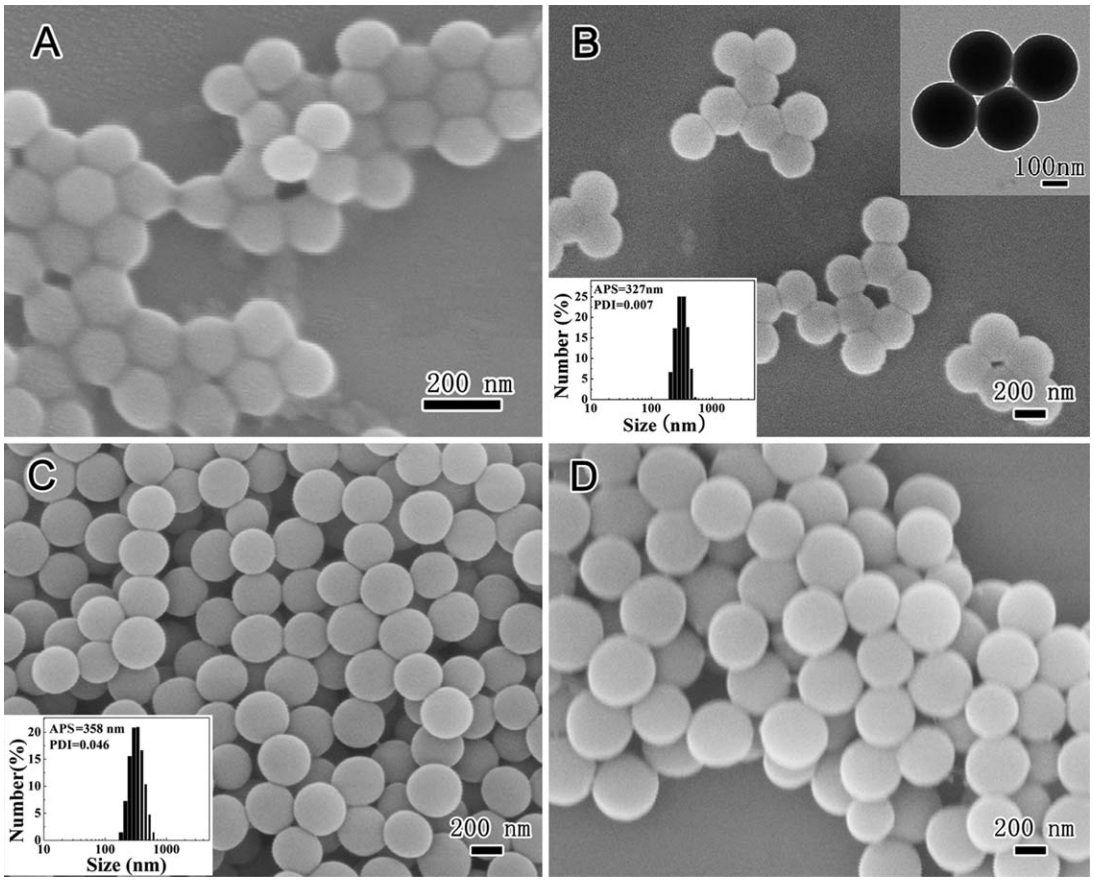

Figure 2. SEM micrographs of the WBPU/PS composite particles at the polymerization time of 5 h when the St/WBPU feed weight ratio was (A) 3/1, (B) 10/1, (C) 20/1, and (D) 50/1, respectively. St/DVB was 98/2 (wt/wt). The polymerization temperature was 70°C. The inset in the top right corner of (B) was its TEM image. The insets in the lower left corners of (B) and (C) were each particle size distribution by DLSA.

1(A,B), it is clear that pure WBPU latex particles were not monodispersed because the WBPU aqueous dispersion was acquired by a high speed of mechanical stirring at 1000 rpm. The chemical composition and structure of the WBPU were analyzed by FTIR and ^{1}H NMR (Figure 3).

In this study, to investigate the influence of the St/WBPU feed ratio on morphology of WBPU/PS composite particles, we tested the weight ratio of St/WBPU to be 3/1, 10/1, 20/1, and 50/1, respectively. The SEM images of the WBPU/PS composite particles prepared at varied weight ratios of St with respect to WBPU were correspondingly shown in Figure 2(A–D). Clearly, all the WBPU/PS composite particles at the same polymerization time of 5 h were more or less spherical and monodispersed. The Bragg diffraction light with various colors was observed when all the monodispersed WBPU/PS latexes were coated onto glass slices. To further confirm monodispersity of the composite particle synthesized, as typical examples, the composite particle size distributions collected by dynamic laser scattering analysis (DLSA) are shown in Figure 2(B,C). For the St/WBPU ratio of 10/1 (wt/wt), the APS of composite particles was 327 nm with PDI of 0.007 [Figure 2(B)]. Upon the St/WBPU weight ratio being 20/1, the APS of WBPU/PS composite particles reached 358 nm with PDI of 0.046 [Figure 2(C)]. Therefore, these WBPU/PS composite particles were indeed monodisperse. At the same time, in Figure 2(A), we noted that some isolated WBPU made WBPU/PS composite particles conglutinated each other, which was attributed to thicker layer of the WBPU onto the surface of those composite particles.

As shown in Figure 2, it is clear that the size of the WBPU/PS composite particles increased with higher St/WBPU feed ratio. The largest WBPU/PS composite particles were obtained while the St/WBPU weight feed ratio (50/1) was the highest. The APS of composite particles measured from the SEM images shown in Figure 2 were from about 158 to 393 nm with increasing St/WBPU feed ratio.

In addition, we observed that further polymerization beyond 5 h led to partial agglomeration of the WBPU/PS composite particles. Then, we investigated the influence of polymerization time on emulsion stability of the St/WBPU soap-free polymerization system by means of ζ-potential analysis. As a typical example, the St/WBPU feed ratio of 3/1 (wt/wt) was used in this synthesis at 70°C, and the result is summarized in Table I.

As summarized in Table I, the ζ-potential in absolute value of the St/WBPU system presents the change from gradual increase turning toward decrease with increasing polymerization time. Further, the ζ-potential of absolute value decreased sharply till 5 h, which was consistent with the experimental phenomenon

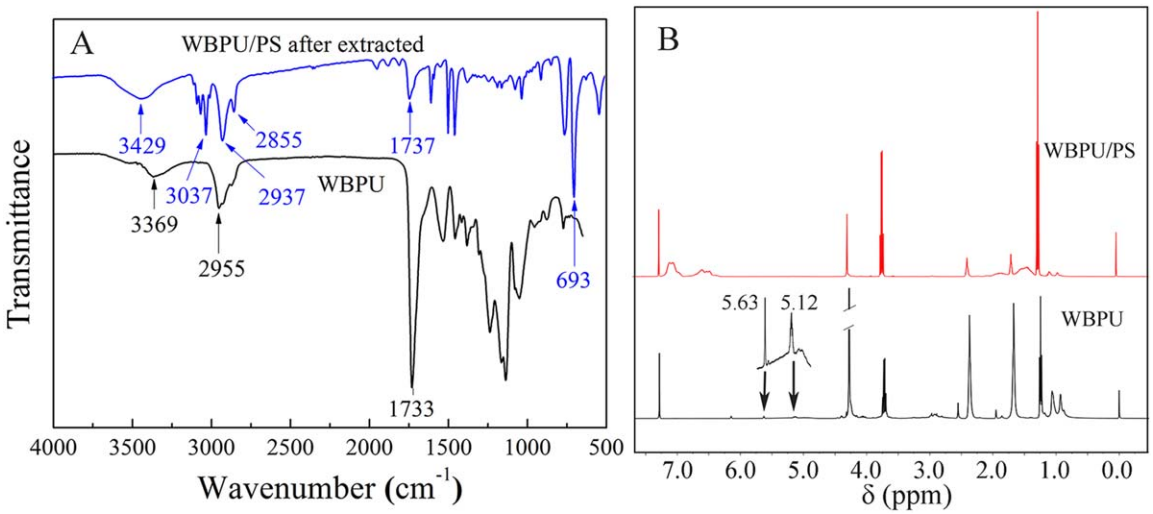

Figure 3. (A) FTIR spectra of the pure WBPU and the remainder after the WBPU/PS composite particles extracted by acetic acid for 72 h; (B) ^{1}H NMR spectra of the pure WBPU and the WBPU/PS composite particles. St/WBPU was 3/1 (wt/wt) and St/DVB was 98/2 (wt/wt). The polymerization time was 5 h and the polymerization temperature was 70°C. [Color figure can be viewed in the online issue, which is available at wileyonlinelibrary.com.]

(little aggregation) observed. Clearly, the ζ-potential in absolute value appeared maximum at 3 h. In other words, the soap-free St/WBPU system was relatively steady within 3–4 h of polymerization. This result is easily understood. At first, the St/WBPU system was certainly unstable, because much amount of St monomer was still dispersing and swelling, which did not reach an equilibrium, as described in Figures 8 and 9. Although at the late polymerization stage, both size and viscosity of the WBPU/PS composite particles increased owing to continued polymerization and high St conversion, causing that the reacting system could eventually become unstable.[25] After considering St conversion, the maximum polymerization time was limited to 5 h. Therefore, polymerization time of 5 h was usually suggested in the synthesis below.

Figure 3(A) shows the FTIR spectrum of pure WBPU. The strong absorption appeared at 1733 cm^{-1}, indicating that carbonyl groups (C═O) existed in the WBPU microbeads. At the same time, the strong absorption with relatively narrow band appeared at 3369 cm^{-1}, confirming the amido presence of carbamate groups (—NHCOO—). Unfortunately, the C═CH$_2$ characteristic absorption band derived from DMAEMA (theoretically 5.85 wt % content in the WBPU) could not be found in the FTIR spectrum. We attributed this to be too low content of the C═CH$_2$ group (theoretically 0.97 wt % content) in the WBPU. Thus, determinging whether grafting between WBPU and PS happened or not could not be confirmed. In this case, we chose an alternative method.

The WBPU/PS composite particles prepared with 3/1 of St to WBPU weight ratio was extracted by acetic acid[31] for 72 h using Soxhlet's apparatus to remove the WBPU physically absorbed onto the PS, then washed with distilled water at least three times, and dried in vacuum at 40°C. The remainder after the extraction was determined by FTIR as shown in Figure 3(A). The absorption peak at 3429 cm^{-1} assigned to —NHCOO— of WBPU was clearly seen. The peak at 1737 cm^{-1} assigned to carbonyl group was also found. The band at 3037 cm^{-1} was assigned to unsaturated C—H vibration absorption of benzene ring. The abovementioned results indicated that the graft reaction probably happened in this system. Still, one doubt remains that this relatively broad peak at about 3429 cm^{-1} might come from the —OH of trace amount of water which was used in the preparation step.

To further clarify this graft issue, ^{1}H NMR technique was utilized to determine the vinyl group of DMAEMA in the WBPU and WBPU/PS composite particles.It should be noted that cosslinked PS should be removed in preparing the WBPU/PS NMR sample. The ^{1}H NMR spectra of both samples are shown in Figure 3(B). A very weak signal of C═CH$_2$ stemmed from DMAEMA was found at chemical shift (δ) 5.0–6.0 ppm (see arrow and locally magnified picture in Figure 3(B)). At same condition, no resonance peak at δ 5.0–6.0 ppm was seen for the WBPU/PS composite particles. The signal at $\delta = 7.1$ ppm was attributed to the hydrogen resonance of benzene ring. Then, the ^{1}H NMR result further confirmed the occurrence of PS grafting WBPU. The chemical structure of grafting reaction is included together in Scheme 1.

It was necessary for us to reveal the structure of WBPU/PS composite particles. The TEM photographs of the ultrathin cross-sections of the WBPU/PS composite particles stained with OsO_4 vapor for 2 h are shown in Figure 4. In the ultramicrotoming process, the ultrathin cross-sections obtained from different cutting directions and positions led to the different section sizes. As shown in Figure 4, much clearly from the inset in Figure 4, the ultrathin shell of composite particles was darker than the core. Then, we realized that the shell was WBPU and the core was PS, because WBPU was more easily stained by OsO_4 than PS.[32] Upon the WBPU used as seed, the morphology of WBPU/PS composite particles showed complete reverse core–shell structure and the PS presented such homogenous phase. Naturally, it was thought what was the driving force for St

Table I. ζ-Potential of Reaction Systems Versus Polymerization Time

St/WBPU system	Polymerization time (h)	1	2	3	4	5
	ζ-Potential (mV)	−17.9	−27.5	−35.2	−32.0	−15.4
MMA/(WBPU/PS) system	ζ-Potential (mV)	−22.6	−22.9	−24.2	−26.9	−26.3

Note: The ζ-potential of pure WBPU was −40.2 mV. The polymerization temperature was 70°C. Each feed ratio of St/WBPU and MMA/(WBPU/PS) was 3/1 (wt/wt), and St/DVB or MMA/DVB = 98/2 (wt/wt).

penetration into WBPU forming the reverse core–shell particles. This will be explained in detail in the following paragraphs (the description, Figure 11).

To further confirm the reverse core–shell structure, we utilized XPS which was highly surface specific with detecting the depths of a few nanometers and often useful for the acquisition of surface information of composite particles.[33]

Figure 5 shows the XPS spectra of the surface of the WBPU/PS composite particles. It was evident that the N_{1s} spectrum was detected on the surface of the WBPU/PS composite particles, and the content of N was 2.78% as shown in Figure 5(A). For the pure WBPU, the theoretical content of N was 3.68%. The difference obtained from the PS phase is involved in the calculation based on the detection depth of XPS. The high-resolution XPS spectrum of nitrogen atom of the WBPU/PS composite particles in the range of 396–410 eV is shown in Figure 5(B). The nitrogen (N_{1s}) vibrational band appeared at 399.78 eV, which represented the —NHCOO— and —NH— groups in the WBPU/PS composite particles. The above detected results are in accordance with the morphology of the ultrathin cross-sections of the WBPU/PS composite particles observed by TEM (Figure 4). On the basis of the abovementioned results, we concluded that the St monomer polymerized inside the WBPU latex particles subsequently formed PS as the core, whereas the WBPU as the shell. In other words, WBPU latex particles as microreactors were used for the polymerization of St monomer.

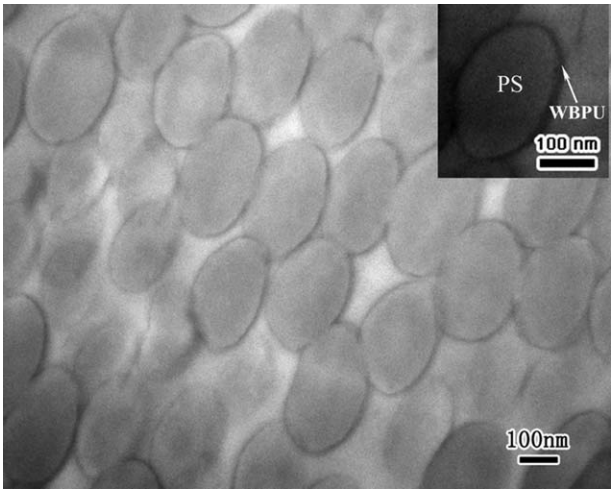

Figure 4. TEM photograph of the ultrathin cross-sections of WBPU/PS composite particles stained with OsO_4 vapor for 2 h. The inset was the highlighted TEM image of one particle for showing clear core–shell structure. The St/WBPU feed ratio was 20/1 (wt/wt) and St/DVB = 98/2 (wt/wt). The polymerization time was 5 h. The polymerization temperature was 70°C.

Morphology of WBPU/PMMA and (WBPU/PS)/PMMA Composite Particles

The overall synthesis procedure could be applicable to another monomer such as MMA. In Figure 6, the WBPU/PMMA composite particles were also monodispersed from TEM analysis.

Submicron-sized peanut-shaped PMMA/PS particles were successfully synthesized by emulsifier-free seeded emulsion polymerization.[34] The nonspherical colloidal particles formed are obtained from phase separation mechanism. It is well known that PMMA was immiscible with crosslinked PS. Here, the (WBPU/PS)/PMMA composite particles were smoothly prepared, whereas the WBPU/PS latex was used for seed latex. The synthetic procedure was the same as the WBPU/PS composite particles. In this study, the MMA/(WBPU/PS) weight ratio was fixed as 3/1. With the aid of SEM observation, the prepared (WBPU/PS)/PMMA composite particles appeared monodispersed spherical instead of peanut shaped as shown in Figure 7(A). Similarly, the TEM image in the inset of Figure 7(B) shows the good monodispersity of the (WBPU/PS)/PMMA particles. According to this phenomenon, no formation of the peanut-shaped structure should be affected by the existence of WBPU. According to the literature, PMMA was compatible with polyurethane. Therefore, the copolymerization of MMA could be facilely performed in the presence of WBPU/PS seed latex.[35] The ζ-potential change of the reaction system as a function of polymerization time is summarized in Table I.

As the TEM micrograph in Figure 7(B) shows, the ultrathin cross-sections of the (WBPU/PS)/PMMA composite particles clearly presented multilayered morphological structure although the ultrathin cross-sections made from different cutting directions led to different sizes and shapes. Here, the PS phase selectively stained by OsO_4 appeared to be black, whereas the PMMA phase was left to be white. It should be noted that the WBPU region is not easy to observe because of the ultrathin WBPU coating and compatibility with PMMA in the (WBPU/PS)/PMMA composite particles (inset in Figure 4, Figure 5).

Recently, many elegant and interesting strategies to synthesize layer-by-layer structure were reported.[36] Now, we can utilize emulsifier-free WBPU particles as microreactors to easily synthesize layer-by-layer particles.

Formation Mechanism of Monodisperse Particles

When the St/WBPU feed ratio was 10/1 (wt/wt), the morphology evolution of the WBPU/PS composite particles during polymerization was studied by sampling aliquots at different time

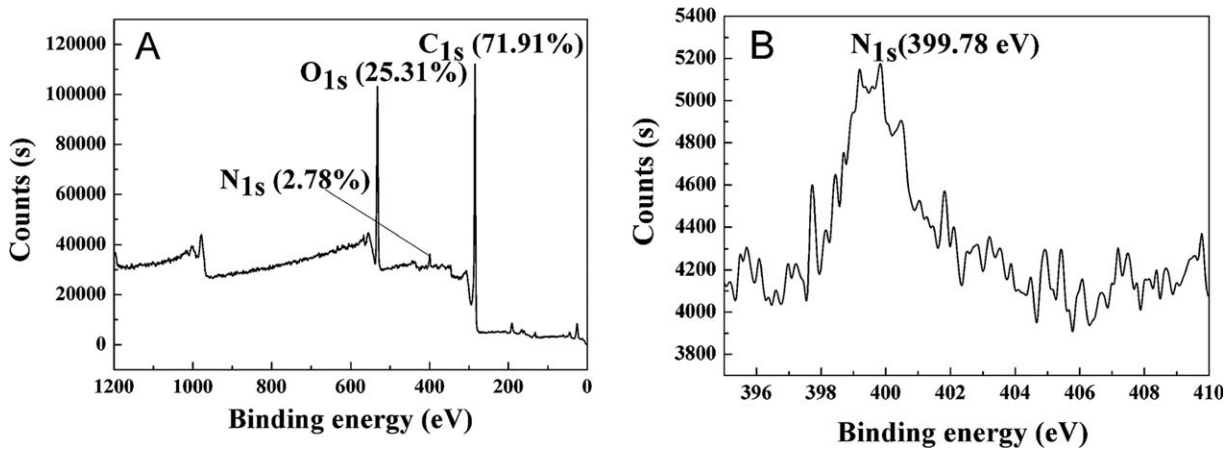

Figure 5. (A) XPS spectrum of WBPU/PS composite particles and (B) high-resolution XPS spectrum of the nitrogen for WBPU/PS composite particles. The St/WBPU feed ratio was 10/1 (wt/wt) and St/DVB = 98/2 (wt/wt). The polymerization time was 5 h. The polymerization temperature was 70°C.

intervals. All samples were dried in reduced pressure to remove any volatile materials (including St monomer), and then observed by SEM; the results are shown in Figure 8.

At 1 h [Figure 8(A)], the WBPU/PS composite particles were inhomogeneous because the WBPU colloidal particles were not monodispersed and little St monomer swelled into the WBPU colloidal particles. Here, the SEM image was fuzzy because oligomers formed at the beginning stage of St polymerization shielded part of electron beam. At 2 h [Figure 8(B)], the WBPU/PS composite particles were not very uniform either. The sample particles looked like gauze covering owing to the abovementioned reason. It can be seen that the conglutination happened between the composite particles owing to the higher content of WBPU within 1–2 h of polymerization time (i.e., at unstable stage; Table I). It should be noted that the WBPU/PS composite particles became larger than before, and smaller particles grew faster. Compared with the composite particles in Figure 8(A), the size difference between larger particles and smaller particles decreased. When the polymerization time reached 3 h, the WBPU/PS composite particles were nearly uniform (Figure 8(C) and Table II). With continuance of the polymerization time to 5 h, the WBPU/PS composite particles became monodispersed [Figure 8(D)]. To make size evolution of the composite particles clearer, the APS of WBPU/PS composite particles obtained by DLSA are also summarized in Table II, corresponding with those latex samples shown in Figure 8. As summarized in Table II, after St polymerizing for 3 h, the composite particles had indeed become monodispersed (because of the PDI at 3 h < 0.05).

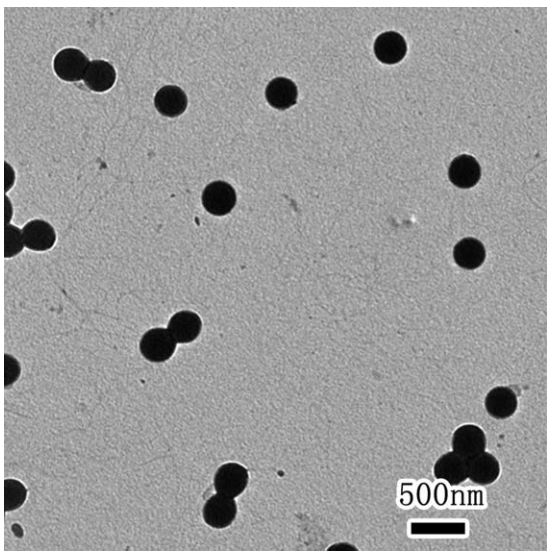

Figure 6. TEM micrograph of the WBPU/PMMA composite particles at the polymerization time of 5 h, MMA/WBPU = 20/1 (wt/wt), and MMA/DVB = 98/2 (wt/wt). The polymerization temperature was 70°C.

We also followed the preparation process for the WBPU/PS composite particles as shown in Figure 9. The polymerization reaction was carried out at 70°C in a 250-mL four-necked round-bottomed flask. About 6 mL of the WBPU/PS latex sampled at a preset time interval without special purification was put into 10 mL of glass bottle to obtain photograph. Clearly, the amount of St monomer, which was oil-like transparent liquid to locate on the top layer in the bottles [Figure 9(A–D)], decreased with the increase of polymerization time. The St monomer almost disappeared after polymerizing for 4 h [Figure 9(D)]. It indicated that little St monomer swelled into WBPU colloidal particles at the initial stage of polymerization. During the polymerization process, St monomer gradually diffused into the latex particles and more monomers diffused into smaller particles owing to higher polymerization rate derived from lower surface charge density. With respect to this point, a detailed depiction will be presented in following text. If each particle were swollen into same amount of St, the size of the composite latex particles should be nonuniform.

The APS of the WBPU/PS composite particles and their PDI versus polymerization time at different St/WBPU feed ratios were tested by Zeta-Sizer 90 type of particle size analyzer (Malvern). The experimental results are shown in Figure 10. As shown in Figure 10(A), all in all the size increased with the extension of polymerization time. It should be noted that the sizes of WBPU/PS composite particles decreased within 2 h of polymerization time. This was because the space of WBPU-hydrated H_2O

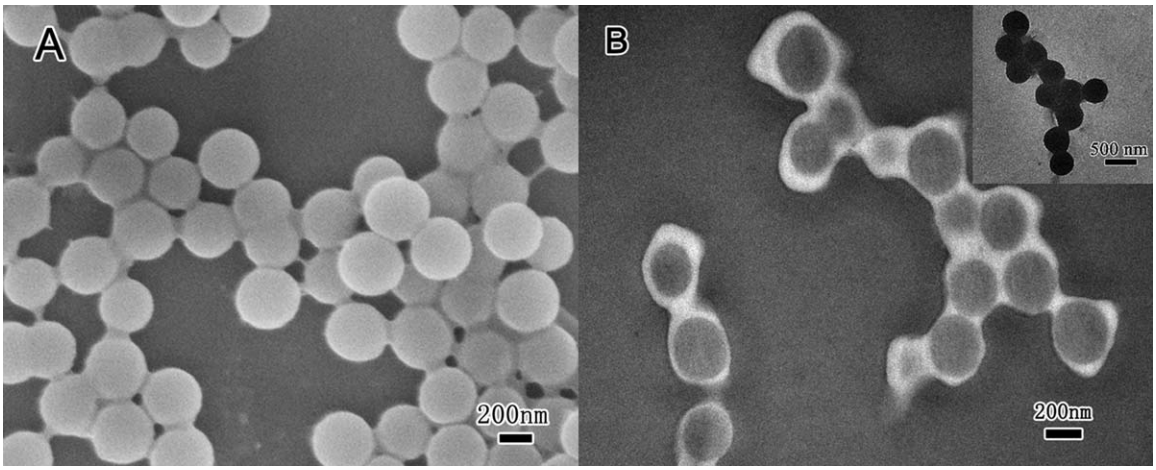

Figure 7. (A) SEM micrograph of and (B) TEM photograph of ultrathin cross-sections of (WBPU/PS)/PMMA composite particles stained with OsO_4 vapor for 2 h, WBPU/St = 1/20 (wt/wt), St/DVB = 98/2 (wt/wt), (WBPU/PS)/MMA = 1/3 (wt/wt), and the inset in (B) is the TEM image without ultrathin section. The polymerization time was 5 h and the polymerization temperature was 70°C.

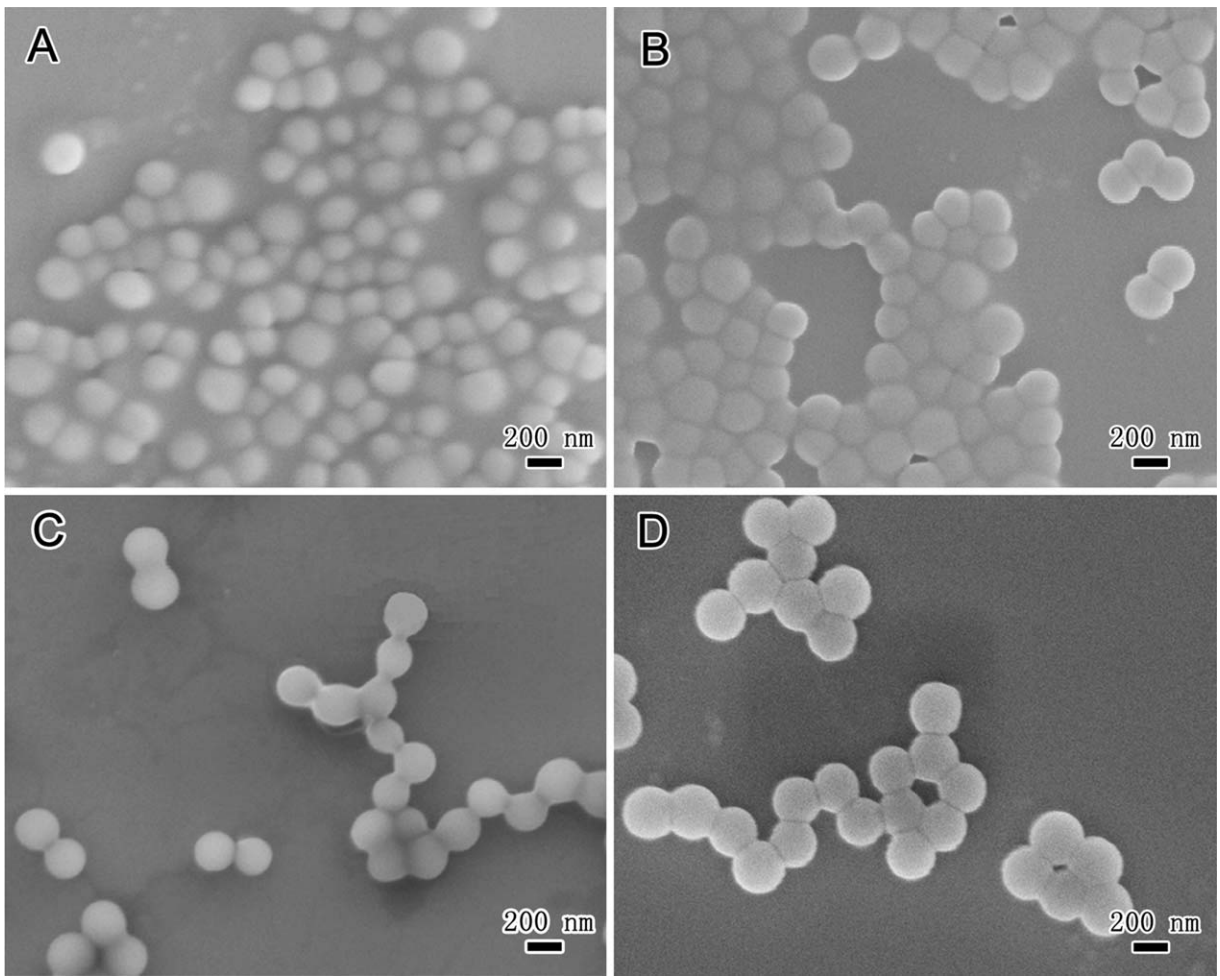

Figure 8. SEM micrographs of the WBPU/PS composite particles at the polymerization time of (A) 1 h, (B) 2 h, (C) 3 h, and (D) 5 h when the St/WBPU feed ratio was 10/1 (wt/wt) and St/DVB = 98/2 (wt/wt). The polymerization temperature was 70°C.

Figure 9. Photographs of the WBPU/PS emulsion at the polymerization time of (A) 1 h, (B) 2 h, (C) 3 h and (D) 4 h when the St/WBPU feed ratio was 10/1 (wt/wt) and St/DVB = 98/2 (wt/wt). The polymerization temperature was 70°C.

molecules, which derived from the hydrophilic groups embedded in pristine WBPU particles, was substituted by St/PS oligomers or droplets, resulting in the shrinkage. The driving force that the St/PS occupying the water space came from its hydrophobic property. At 3 h of polymerization, the overall particle size reached ~287 nm.

Figure 10(B) shows that the PDI of WBPU/PS particles gradually decreased with increasing polymerization time upon St/WBPU feed weight ratio being 10/1 (Table II). At the same time, it can be clearly noticed that when St/WBPU feed ratio was 50/1 (wt/wt), the curve of PDI versus polymerization time had a turning point at 3 h. After 3 h of polymerization, the PDI significantly increased. As we know, with further increasing the polymerization time, few composite particles produced partial agglomeration because of the thin WBPU layer leading to the reduced hydrophilic ability and emulsification. This result was consistent with change trend of the ζ-potential summarized in Table I. Indeed, too large particle size influenced the stability of the latex system, thus resulting in greater PDI. The phenomenon was also supported by the SEM observation on the same sample. With the greater PDI contrary, the SEM image in Figure 2(D) shows that the composite particles were all but monodispersed. We concluded that the higher PDI was largely caused by a little agglomeration of the composite particles with larger size.

Table II. APS of WBPU/PS Composite Particles Versus Polymerization Time

Polymerization time (h)	1	2	3	5
APS (nm)	250.9	262.4	286.6	327.2
PDI	0.112	0.08	0.023	0.007

Note: The St/WBPU feed ratio was 10/1 (wt/wt) and St/DVB = 98/2 (wt/wt). The polymerization temperature was 70°C.

Additionally, a special explanation was given that, at 10/1 (wt/wt) of St/WBPU ratio, the size of the particles at 5 h in Figure 10(A) was in disagreement with that in Figure 2(B), because the composite particles in Figure 2(B) were observed in dried state. Correspondingly, those in Figure 10(A) dispersed in distilled water showed larger size with unreacted monomer and hydrate.

On the basis of the above experimental observations and results, we propose a formation mechanism of the monodisperse particles as shown in Figure 11. We used yellow drops to represent the St monomer and blue drops to represent the WBPU particles (Path 1). During the monomer swelling stage, the St monomer swelled the WBPU particles, whereas the St monomer penetrated into the interior of the WBPU particles. The reason for causing this result was first because the solubility of St in water was so low (ca. 0.37 g/L). The interfacial tension between the St droplets and water was much greater than the interfacial tension between the WBPU particles and water owing to hydrophilicity of the WBPU. Eventually, the St monomer did not dewet the surface of the WBPU particles for the reasons of hydrophilic groups locating on the surface of the WBPU particles (Path 2). Consequently, St monomer was forced to alternatively penetrate into the WBPU particles' interior with reletively hydrophobic surrounding.[37–40] In addition, as reported by Kim and Suh,[41] the swelling of monomer took at least 6 h to reach the equilibrium. In our study, the swelling time was only 2 h, and hence it did not reach the equilibrium. After initiated St polymerization, newly formed PS phase grew by absorption of monomer from the seed phase and around the seeds, because a lower free energy of mixing in the new domain than in the seeds or other domains was the driving force for the transport of monomer (Figure 9).[37–40]

At the initial polymerization stage, more free radicals entered into smaller WBPU particles (Path 3). As the smaller particles had lower surface charge density than the larger particles, charged free radicals were more easily absorbed by them from the water phase.

For example, in the case of two different sizes of particles, if the average number of polymer chains and hydrophilic groups per unit volume in two particles was the same, all hydrophilic groups were located on the particle surface. We assumed the radius of smaller particle (r) the radius of larger particle ($2r$), the number of polymer chain of smaller particle (N), and the number of hydrophilic group of smaller particle (αN). Then, the hydrophilic surface charge densities on two particles were calculated using the following set of equations[42]:

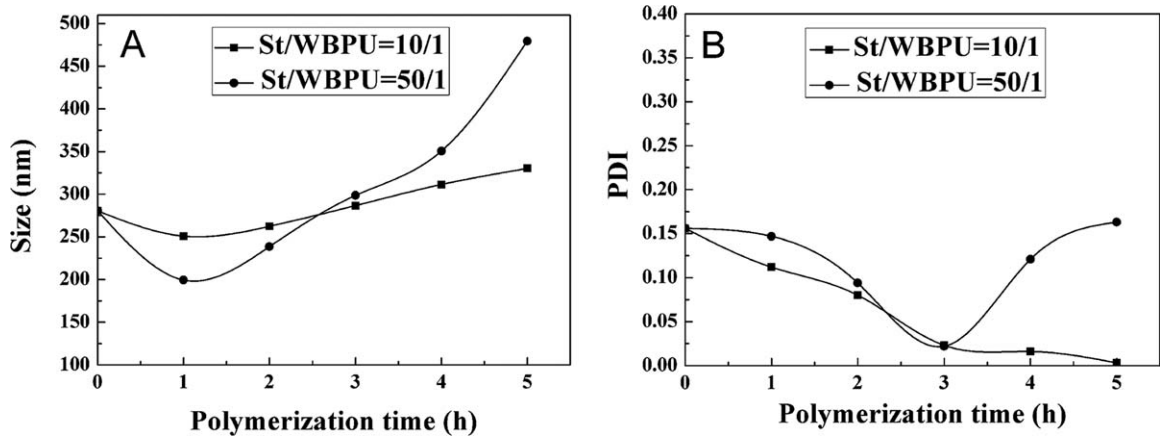

Figure 10. (A) Average size of WBPU/PS composite particles and (B) PDI versus polymerization time when the St/WBPU feed ratio was 10/1 (wt/wt), 50/1 (wt/wt), and the St/DVB feed ratio was 98/2 (wt/wt). The polymerization time was 5 h. The polymerization temperature was 70°C.

$$S_S = 4\pi r^2$$

$$S_L = 16\pi r^2$$

$$V_S = \frac{4}{3}\pi r^3$$

$$V_L = \frac{32}{3}\pi r^3 = 8\left(\frac{4}{3\pi r^3}\right)$$

Hence, the number of polymer chain of larger particle, is $8N$; the number of hydrophilic group of larger particle is $8\alpha N$.

$$D_S = \frac{\alpha N}{4\pi r^2}$$

$$D_L = \frac{8\alpha N}{16\pi r^2} = \frac{\alpha N}{2\pi r^2}$$

where S_L and S_S were the superficial area of larger particle and smaller particle, respectively; V_L and V_S were the volume of larger particle and smaller particle, respectively; D_L and D_S were the hydrophilic surface charge density of larger particle and smaller particle, respectively; α was proportional constant. Apparently, the smaller particle had the lower hydrophilic surface charge density.

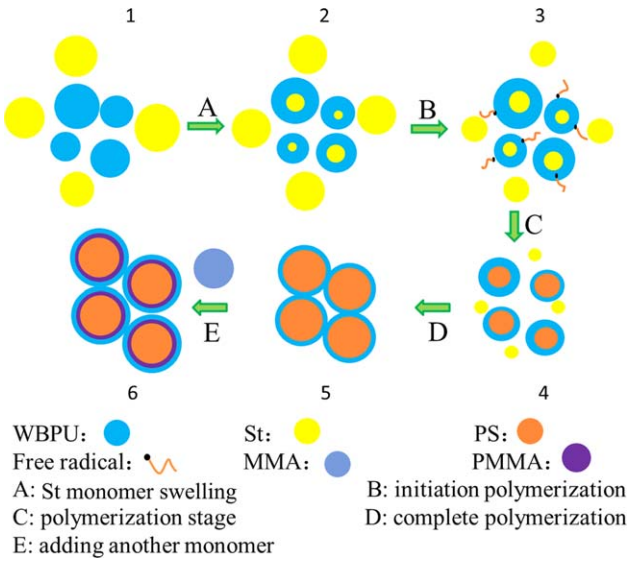

Figure 11. Schematic morphology evolution of the WBPU/Polymer colloidal particles during emulsifier-free batch-seeded emulsion polymerization. [Color figure can be viewed in the online issue, which is available at wileyonlinelibrary.com.]

But in conventional emulsion polymerization, emulsifier molecules were physically adsorbed on the surface of the particles. Regardless of how big the particles were, the surface charge density tended to be the same. Large particle had higher average number of free radical and faster growth rate than small particle, which can cause the differentiation in particle size. Hence, emulsifier-free emulsion polymerization was easier to get monodisperse latex particles.[42]

As the polymerization process continued, the WBPU/PS composite particles (red to represent PS phase) became bigger, the St monomer became less until St monomer drops disappeared gradually. The composite particles became monodispersed gradually (Paths 4 and 5). At the same time, the particle size increased and the St monomer conversion improved. On the basis of this mechanism, the polymerization could be continued. Another monomer could be introduced to this synthesis procedure such as MMA (purple to represent it) to form multilayered core–shell structure of composite particles (Path 6, dark purple to represent PMMA phase).

Dynamic Mechanical Performance of Composite Particles

Figure 12(A) shows the temperature-dependent storage modulus of WBPU, WBPU/PS, and (WBPU/PS)/PMMA samples. The storage modulus of all the three samples decreased as temperature increased. Their storage modulus decreased steeply beginning at their corresponding glass transition temperature (T_g) regions, except for the modulus change of the (WBPU/PS)/PMMA sample in low-temperature transition range. Clearly, the modulus of (WBPU/PS)/PMMA sample was much higher than that of the WBPU/PS sample which was much higher than that of the WBPU. This great difference largely depends on the composition proportion in the WBPU/PS and (WBPU/PS)/PMMA samples. The former was 37/63 (wt/wt) and the latter was 12/

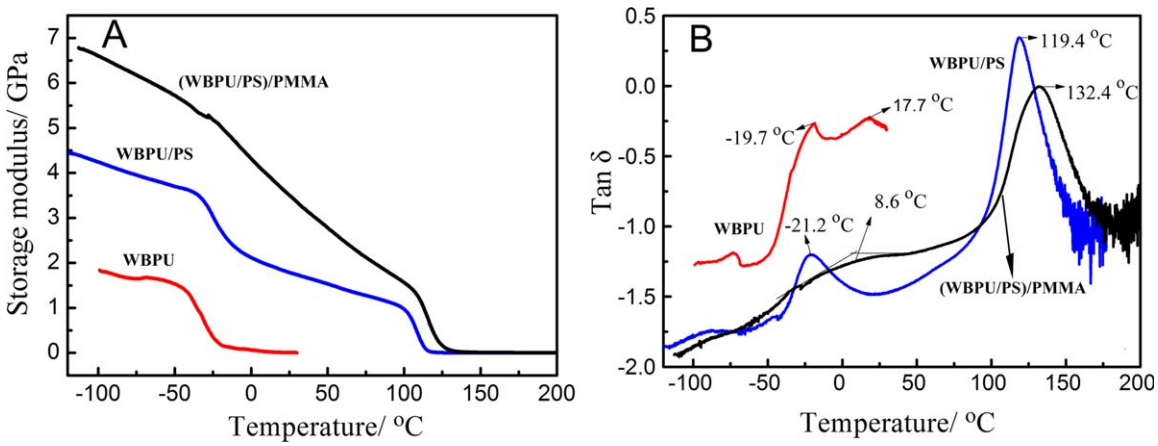

Figure 12. (A) Storage modulus and dynamic mechanical loss tangent (tan δ) of WBPU, WBPU/PS, and (WBPU/PS)/PMMA samples as a function of temperature. St/WBPU or MMA/(WBPU/PS) feed ratio was 3/1 (wt/wt), and St/DVB or MMA/DVB = 98/2 (wt/wt). The polymerization was performed at 70°C for 5 h. [Color figure can be viewed in the online issue, which is available at wileyonlinelibrary.com.]

22/66 (wt/wt/wt), which were calculated by analysis of nitrogen and carbon content in these samples.

Figure 12(B) shows the changes of the dynamic mechanical loss tangent (tan δ) of WBPU, WBPU/PS, and (WBPU/PS)/PMMA samples as a function of temperature. Here, T_g was considered as a peak temperature of tan δ. For the WBPU sample, there were two peak temperatures of tan δ (−19.7, 17.7°C, respectively) which was attributed to respective T_gs of soft segment and hard segment. For the WBPU/PS sample, there were also two peak temperatures of tan δ (−21.2, 119.4°C, respectively) which assigned to the T_gs of corresponding WBPU and PS. The enhanced T_g (119.4°C) of PS, in comparison with linear PS (T_g, ca. 100°C), was owing to the PS crosslinked. The T_g (−21.2°C) in low-temperature range for the WBPU/PS was slightly lower than that of WBPU (−19.7°C). This might be caused by the occurrence of worse phase separation between WBPU and PS compared with the pure WBPU.

Nevertheless, as for the (WBPU/PS)/PMMA sample, the T_g at 8.6°C in low-temperature range was not obvious, which attributed to the lower content of WBPU (ca. 12 wt %) in the (WBPU/PS)/PMMA composite particles. The partial PS or/and PMMA macromolecular chains diffusing into WBPU layer induced the change profile. Based on the same reason, the sample modulus in Figure 12(A) shows a smooth decrease in the temperature range. In high-temperature range, the peak temperature of tan δ at 132.4°C was much higher than that of pure noncrosslinked PS or PMMA (105–115°C). This is obtained from the crosslinked PS and PMMA, and partly interpenetrating networks of structure between PS and PMMA.[43,44]

CONCLUSIONS

We have demonstrated a flexible and versatile approach for the synthesis of monodisperse composite particles with submicron sizes. The monodispersed WBPU/PS composite particles were obtained by emulsifier-free batch-seeded emulsion polymerization of St monomer in water media using WBPU as microreactors. It is reasonably believed that the WBPU located on the surface of PS particles according to the XPS detection results and the TEM photographs with the ultrathin cross-sections of WBPU/PS composite particles. Furthermore, the multilayered (WBPU/PS)/PMMA composite particles were successfully synthesized. On the basis of the above experimental results, the formation mechanism of monodisperse particles was proposed that smaller particles have lower surface charge density than larger particles, and charged free radicals are more easily absorbed by the smaller particles from the water phase. Thus, the smaller particle has higher average number of free radicals and faster growth rate than the larger particle. Consequently, emulsifier-free emulsion polymerization is easier to achieve monodisperse latex particles in comparison with conventional emulsion polymerization.

The individual properties of composite particles could be tailored by changing average sizes and compositions such as feed ratio, polymerization time, and monomer type. Here, a variety of functional comonomers could be introduced by active polyaddition reaction in the preparation of WBPU to program the synthesis of composite particles. Therefore, core–shell particles with ideal multifunctional structures could be achieved intriguingly by using WBPU microreactors. These novel monodisperse composite particles may have great potentials for modifying agent and functional coating applications.

ACKNOWLEDGMENTS

The authors acknowledge the support for this study from the Hebei Province Natural Science Fund (B2012202131) and the National Natural Science Foundation of China (Project no. 51373047). The authors thank Dr. X.S. Feng and Dr. Z. Li for helpful discussions.

REFERENCES

1. Xu, X. L.; Asher, S. A. *J. Am. Chem. Soc.* **2004**, *126*, 7940.
2. Xia, Y. N.; Gates, B.; Yin, Y. D.; Lu, Y. *Adv. Mater.* **2000**, *12*, 693.
3. Nakamura, H.; Ishii, M.; Tsukigase, A.; Harada, M.; Nakano, H. *Langmuir* **2005**, *21*, 8918.

4. Jin, Y.; Zhu, Y. H.; Yang, X. L.; Jiang, H. B.; Li, C. Z. *J. Colloid Interface Sci.* **2006**, *301*, 130.
5. Lunelli, L.; Pasquardini, L.; Pederzolli, C.; Vanzetti, L.; Anderle, M. *Langmuir* **2005**, *21*, 8338.
6. Zhang, Y. J.; Wang, X. H.; Wang, Y. X.; Liu, H. L.; Yang, J. H. *J. Alloy Comp.* **2008**, *452*, 473.
7. Zhang, Y. J.; Li, W.; Chen, K. J. *J. Alloy Comp.* **2008**, *450*, 512.
8. Wang, S. J.; Wang, X. B.; Zhang, Z. C. *Eur. Polym. J.* **2007**, *43*, 178.
9. Chen, J.; Zhang, Z. C.; Zhang, Q. F. *Radiat. Phys. Chem.* **2009**, *78*, 906.
10. Reese, C. E.; Asher, S. A. *J. Colloid Interface Sci.* **2002**, *248*, 41.
11. Du, X.; He, J. H. *J. Appl. Polym. Sci.* **2008**, *108*, 1755.
12. Pargen, S.; Willems, C.; Keul, H.; Pich, A.; Möller, M. *Macromolecules* **2012**, *45*, 1230.
13. Zhang, Q.; Han, Y.; Wang, W. C.; Song, T.; Chang, J. *J. Colloid Interface Sci.* **2010**, *342*, 62.
14. Horák, D. *J. Polym. Sci. Part A: Polym. Chem.* **2001**, *39*, 3707.
15. Shim, S. E.; Jung, H.; Lee, K.; Lee, J. M.; Choe, S. *J. Colloid Interface Sci.* **2004**, *279*, 464.
16. Kim, S. Y.; Lee, K.; Jung, H.; Shim, S. E.; Lee, B. H.; Choe, S. *Polymer* **2005**, *46*, 7974.
17. Song, J.-S.; Winnik, M. A. *Macromolecules* **2005**, *38*, 8300.
18. Okubo, M.; Izumi, J.; Takekoh, R. *Colloid Polym. Sci.* **1999**, *277*, 875.
19. Li, X.; Zuo, J.; Guo, Y. L.; Yuan, X. H. *Macromolecules* **2004**, *37*, 10042.
20. Song, J.-S.; Chagal, L.; Winnik, M. A. *Macromolecules* **2006**, *39*, 5729.
21. Limé, F.; Irgum, K. *Macromolecules* **2009**, *42*, 4436.
22. Song, J.-S.; Tronc, F.; Winnik, M. A. *J. Am. Chem. Soc.* **2004**, *126*, 6562.
23. Xu, S. Q.; Nie, Z. H.; Seo, M.; Lewis, P.; Kumacheva, E.; Stone, H. A.; Garstecki, P.; Weibel, D. B.; Gitlin, I.; Whitesides, G. M. *Angew. Chem. Int. Ed.* **2005**, *44*, 724.
24. Tan, J. B.; Wu, B.; Yang, J. W.; Zhu, Y. D.; Zeng, Z. H. *Polymer* **2010**, *51*, 3394.
25. Pan, M. W.; Yang, L. Y.; Guan, B.; Lu, M. S.; Zhong, G. J.; Zhu, L. *Soft Matter* **2011**, *7*, 11187.
26. Wang, S. J.; Zhang, G. X.; Zhang, Z. C.; Zou, M. X. *Colloid Surf. A: Physicochem. Eng. Asp.* **2007**, *298*, 158.
27. Zhang, G. X.; Zhang, Z. C.; Xu, C. Q.; Ye, Q. *Colloid Surf. A: Physicochem. Eng. Asp.* **2006**, *276*, 72.
28. Zhang, G. X.; Zhang, Z. C.; Hu, Z. Q.; Xi, H. X. *Colloid Surf. A: Physicochem. Eng. Asp.* **2005**, *264*, 37.
29. Mbenkum, B. N.; Díaz-Ortiz, A.; Gu, L.; van Aken, P. A.; Schütz, G. *J. Am. Chem. Soc.* **2010**, *132*, 10671.
30. Buxton, G. A.; Balazs, A. C. *Mol. Simul.* **2004**, *30*, 249.
31. Kim, S. H.; Son, W. K.; Kim, Y. J.; Kang, E.-G.; Kim, D.-W.; Park, C. W.; Kim, W.-G.; Kim, H.-J. *J. Appl. Polym. Sci.* **2003**, *88*, 595.
32. Zhu, Y.; Sun, D. X.; Li, N.; Jiang, W. R. *Petrochem. Technol.* **2003**, *32*, 796.
33. Yang, C. L.; Guan, Y. P.; Xing, J. M.; Liu, H. Z. *Langmuir* **2008**, *24*, 9006.
34. Shi, S.; Wang, T.; Tang, Y. T.; Zhou, L. M.; Kuroda, S. I. *Chinese Chem. Lett.* **2011**, *22*, 1127.
35. Nair, P. D.; Krishnamurthy, V. N. *J. Appl. Polym. Sci.* **1996**, *60*, 1321.
36. Caruso, F. *Adv. Mater.* **2001**, *13*, 11.
37. Liu, X.; Pan, M. W.; Yuan, J. F.; Niu, Q.; Wang, X. M.; Zhang, K. C. *RSC Adv.* **2014**, *4*, 4163.
38. Sheu, H. R.; El-Aasser, M. S.; Vanderhoff, J. W. *J. Polym. Sci. Part A: Polym. Chem.* **1990**, *28*, 629, 653.
39. Mock, E. B.; Bruyn, H. D.; Hawkett, B. S.; Gilbert, R. G.; Zukoski, C. F. *Langmuir* **2006**, *22*, 4037.
40. Niu, Q.; Pan, M. W.; Yuan, J. F.; Liu, X.; Wang, X. M.; Yu, H. F. *Macromol. Rapid Commun.* **2013**, *34*, 1363.
41. Kim, J.-W.; Suh, K.-D. *Polymer* **2000**, *41*, 6181.
42. Zhang, H. T.; Huang, J. X. Emulsion Polymerization New Techniques and Applications; Chemical Industry Press: Beijing, **2007**, Chaper *4*, p 74.
43. Pan, M. W.; Zhang, L. C. *J. Appl. Polym. Sci.* **2003**, *90*, 643.
44. Pan, M. W.; Zhang, L. C.; Wan, L. Z.; Guo R. Q. *Polymer* **2003**, *44*, 7121.